M.S. THESIS

FABRICATION OF ENCODED MICROPARTICLES FOR ANTI-COUNTERFEITING APPLICATIONS

위조방지기술에 적용가능한 코드화된 미세입자 제작

BY

HYUNG JONG BAE

FEBRUARY 2013

DEPARTMENT OF ELECTRICAL ENGINEERING AND
COMPUTER SCIENCE
COLLEGE OF ENGINEERING
SEOUL NATIONAL UNIVERSITY

M.S. THESIS

FABRICATION OF ENCODED MICROPARTICLES FOR ANTI-COUNTERFEITING APPLICATIONS

위조방지기술에 적용가능한 코드화된 미세입자 제작

BY

HYUNG JONG BAE

FEBRUARY 2013

DEPARTMENT OF ELECTRICAL ENGINEERING AND
COMPUTER SCIENCE
COLLEGE OF ENGINEERING
SEOUL NATIONAL UNIVERSITY

FABRICATION OF ENCODED MICROPARTICLES FOR ANTI-COUNTERFEITING APPLICATIONS

위조방지기술에 적용가능한
코드화된 미세입자 제작

지도교수 권 성 훈

이 논문을 공학석사 학위논문으로 제출함

2012 년 11 월

서울대학교 대학원

전기컴퓨터 공학부

배 형 종

배형종의 공학석사 학위논문을 인준함

2013 년 2 월

위 원 장 : _____박__영__준_____

부위원장 : _____권__성__훈_____

위 원 : _____김__성__재_____

Abstract

The number of counterfeiting crimes, such as counterfeiting of banknotes, drugs, and even liquors, has steadily grown in the global marketplace. Although a lot of anti-counterfeiting methods are applied to products, advanced technologies are required in order to deal with increasingly sophisticated counterfeit crimes. An anti-counterfeiting technique based on microparticles is difficult to copy because they are very small to detect and many different particles can be integrated, but few technologies using microparticles have been developed. In this thesis, I fabricate encoded microparticles and demonstrate applications of this anti-counterfeiting tool, especially suitable for use with banknotes and drugs.

First, shape-coded microparticles are fabricated and applied to banknotes. The size of fabricated polymeric microparticles range from 50㎛ to 500㎛. Special letters are encoded on the different shapes of particles and three different fluorescent dyes are used to realize color information. Since microparticles should be mixed with the paper pulp and printing inks used in the production of banknotes, fabricated polymeric microparticles are silica coated to protect them from the physical stress during the formulation process. Silica-coated microparticles, which have thicknesses

from 15㎛ to 40㎛, are successfully integrated into the paper regardless of their size. Such shape-coded microparticles can provide a high level of added security because they are small and information is coded on a particle by both the shape and the fluorescence. Therefore, they could be utilized as a new anti-counterfeiting tool for banknotes.

Second, QR-coded microparticles, which can be decoded using a smartphone QR code reader application, are synthesized for the anti-counterfeiting of drugs. A fluorescent acrylic monomer is utilized to minimize diffusion of the fluorescent dye from the particle as well as provide high color contrast between the code and backgrounds. According to the simulation results of propagation of the projected ultraviolet light inside the microfluidic channel, the module size of QR code is set at less than 40㎛ with a channel height greater than 25㎛ to prohibit separation of island patterns which exist inside the particle. The encoding capacity of fabricated QR-coded microparticles mainly depends on both the version of QR code and error correction level. Version 7 microparticles with maximum error correction levels are capable of encoding 93 characters, which is sufficient for storing specific drug information such as the name of the manufacturer, the production date, and the expiration date. At the maximum error correction level, damaged codes with up to approximately 20% of the data area degraded are successfully recovered. Also, the code is successfully decoded without alignment between the particle and the

decoding device with the assistance of position detection patterns. The authentication process is demonstrated using a drug capsule containing QR-coded microtaggants and cytotoxicity tests verify that fabricated microparticles are not toxic to cells. Since presented QR-coded microparticles feature high encoding capacities as well as error correction capabilities that were difficult to implement in previous microtaggants, they could be widely used as a part of a highly effective anti-counterfeiting method for drugs.

Keywords: Anti-counterfeiting, Shape-coded microparticle, Silica-coating, QR-coded microparticle

Student Number: 2011-20853

Contents

List of Figures

Chapter 1

Introduction

The problem of counterfeiting has steadily grown in the global market, especially as computer and printing technologies have advanced, it has become much easier to counterfeit currency and as a result the problems have become critical in the global currency market. The problems have occurred not only with money, but with passports, identification cards, official security documents, drugs, and even liquors. To cope with sophisticated crimes of counterfeiting, advanced anti-counterfeiting technologies are required to prevent forgery of commodities.

Optically variable devices (OVDs) are the most widely used tools for anti-counterfeiting of banknotes because people can easily recognize optical visualization. Various techniques utilizing diffraction [1, 2], interference [3], reflection [4], and polarization [5] of the light, holograms [3, 6], and an optical

coating [7] have been developed for security purposes. In addition, watermarks [8], fluorescence material such as a fluorescent fiber [9], and even organic transistors [10] or light-emitting organic nanofibers [11] have also been applied to banknotes. Currently more than fifteen techniques are incorporated in the official Korean notes. However, few anti-counterfeiting techniques utilizing microparticles have been developed and particle-based methods are not used within Korean currency.

Another big counterfeiting market is the medicine market. According to the Center for Medicine in the Public Interest, about 30% of brand name drug sales in developing countries are counterfeit. Since illegally copied drugs can threaten our health and even cause unnecessary deaths, eliminating counterfeit drugs has become an important issue. Packaging-oriented authentication, such as character printing, radio frequency identification (RFID), and optical tags, has been conventionally used in the packaging process [12]. However, these are insufficient for fully authenticating drugs because they are susceptible to forgery. As an alternative technology, on-dose authentication (ODA) which tags an individual unit-of-dose form at the drug formulation level has emerged for anti-counterfeiting of drugs [13, 14]. Microscopic and traceable identification particles known as microtaggants are added to various materials for anti-counterfeiting and have become one of the most powerful tools for ODA because they can be simply incorporated in drugs and it is difficult to copy microscopic particles which have various functions and which

contain various information. For example, microtaggants which consist of polymeric microparticles and microfibers are fabricated for anti-counterfeiting of drugs [15]-[17]. Although microparticles have been utilized in anti-counterfeiting methods for drugs, previously developed microparticles may be insufficient for containing large quantities of data for authenticating drugs because the conventional graphical code schemes, such as one-dimensional (1D) barcodes or letters, were printed on the microparticle. Also, they cannot provide error correction capacity of the data from the damaged areas of the particle.

In this thesis, I present anti-counterfeiting methods for banknotes and drugs using encoded microparticles. Microparticles can be synthesized with various parameters such as size, thickness, shape, and even materials that form the particle itself by using optofluidic maskless lithography (OFML) [18]. All of these parameters can provide a code that can store information inside the particle. Such a lithographically fabricated microparticle platform can provide high encoding capacity because different conditions of each of the parameters can be easily integrated in a particle. Also, it is difficult to copy encoded microparticles because they are very small to detect and particles of different types can be mixed for authentication purposes.

Shape-coded microparticles with fluorescent dye were fabricated for anti-counterfeiting of paper substrates. Since both the shape and the fluorescence color of

the particle function as a code, security levels can be enhanced using various combinations of shapes and fluorescent dyes. Also microparticles can be randomly positioned on the banknote by mixing them with the paper pulp during the manufacturing process. Another option would be positioning microparticles on a selected location by mixing them with the ink that will be applied to the banknote. To this end, such encoded microparticles can be applicable to banknotes as a new, particle-based anti-counterfeiting tool.

Also, microtaggants coded by QR (Quick Response) code were fabricated for anti-counterfeiting of drugs [19]. By patterning QR codes on the microparticles, high-capacity encoding and recovery of data from physically damaged areas of particles was possible, which could provide a high-level verification capability that effectively overcomes the limitations of previous microtaggants.

Chapter 2

Encoded microparticles for anti-counterfeiting of banknotes

In Chapter 2, I introduce the fabrication process of polymer microparticles and demonstrate application of shape-coded microparticles with a fluorescent dye for anti-counterfeiting of banknotes.

2.1 Optofluidic maskless lithography (OFML)

The OFML is a flow lithography technique that can dynamically synthesize free-floating polymeric microstructures inside microfluidic channels. As shown in Figure 2.1, this system consists of a digital micromirror device (DMD), an ultraviolet (UV) light source, a microfluidic channel for stream of UV-curable polymer, and a microscopic imaging system for inspection and monitoring. By combining the concept of programmable optical projection using DMD and continuous flow

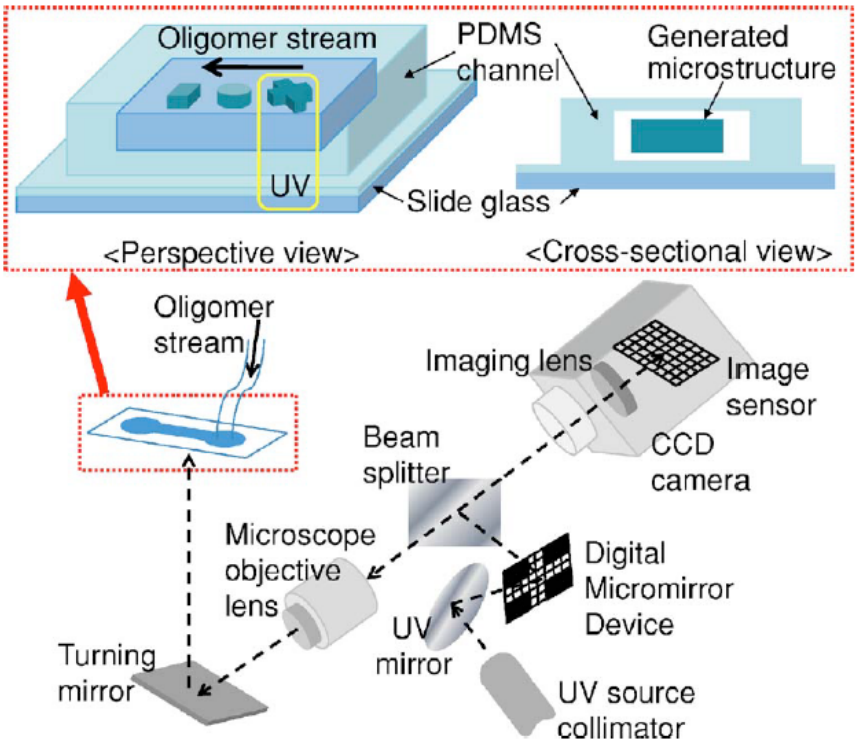

Figure 2.1 Schematic diagram of the proposed optofluidic maskless lithography system for dynamic control of the photopolymerization process in microfluidic devices [18].

lithography techniques within the microfluidic channels, polymeric particles of various shapes and sizes can be fabricated.

Microfluidic channels used in the OFML system were fabricated by standard soft lithography techniques with polydimethylsiloxane (PDMS) [20]. Oxygen exists near the inner walls of the PDMS channel because PDMS is permeable by oxygen. When the photocurable prepolymer is exposed to the UV light, oxygen prohibits the

polymer from polymerizing near PDMS surfaces because of the quenching of free radicals by oxygen. This oxygen inhibition layer allows fabrication of free floating structures [21]. Therefore, shape-coded microparticles can be fabricated continuously in the microfluidic channels by selectively solidifying photocurable resin using DMD mask patterns.

To increase resolution of the structures, flow of the polymer should be stopped before beginning UV illumination using a computer controlled solenoid valve system [22]. However, this technique has a disadvantage in productivity of microparticles because flow requires time for stability right after closing of the valve. To overcome this limitation, a “step and repeat” lithography technique was developed by combining two parallel microfluidic channels and a motorized microscope stage with the OFML system [23]. This experimental setup allows high throughput fabrication of different shapes of polymeric microparticles.

2.2 Shape-coded microparticles

Microparticles were developed as a new anti-counterfeiting tool for banknotes. Fabricated microparticles can be integrated in banknotes during the production process of banknotes, and mixed with inks to print on banknotes. I conducted this research with Korea Minting, Security Printing and ID Card Operating Corportation (KOMSCO).

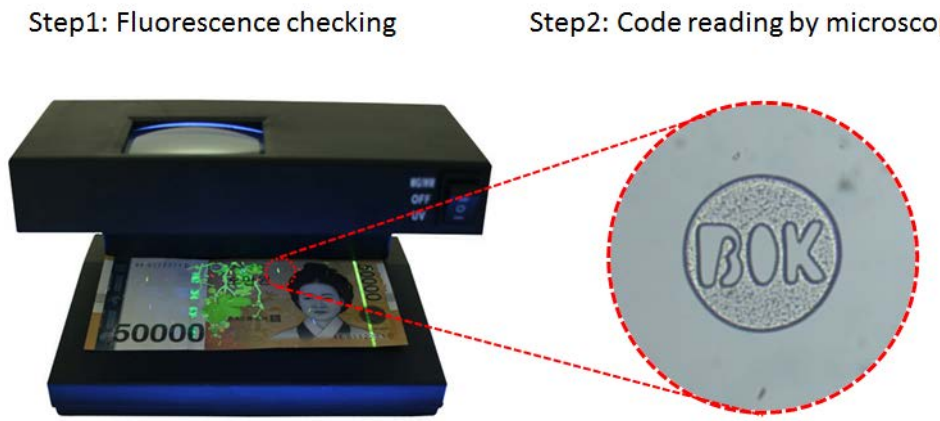

Figure 2.2 The authentication process of banknotes which have shape-coded microparticles. First, identify hidden microparticles by fluorescence emission using an UV illumination device. In the next step, magnify the detected microparticle using a microscope and decode information [24].

The authentication process of banknotes containing microparticles is shown in Figure 2.2. First, banknotes are checked by portable UV illumination device to identify the existence of microparticles using their fluorescence. Then the shape of the particle (which contains information for authentication) is decoded using a microscope. Here, microparticles of various sizes, 50 ~ 500 ㎛, were fabricated as materials for inserting inside banknotes.

In the first method, small particles were fabricated to make it difficult for people to find the particles with the naked eye. Star and circle shaped microparticles with the character “K” were synthesized (Figure 2.3(A) and (B)). Prepolymer resin consisted of poly(ethylene glycol) diacrylate (PEG-DA, Mn=700), a photoinitiator,

and rhodamine B. Since particles contained rhodamine, the existence of the particles could be detected by shining green light in order to excite the dye. Then the shapes of the particles, both the outer shape and the inside characters, were decoded by magnifying the particles using a microscope.

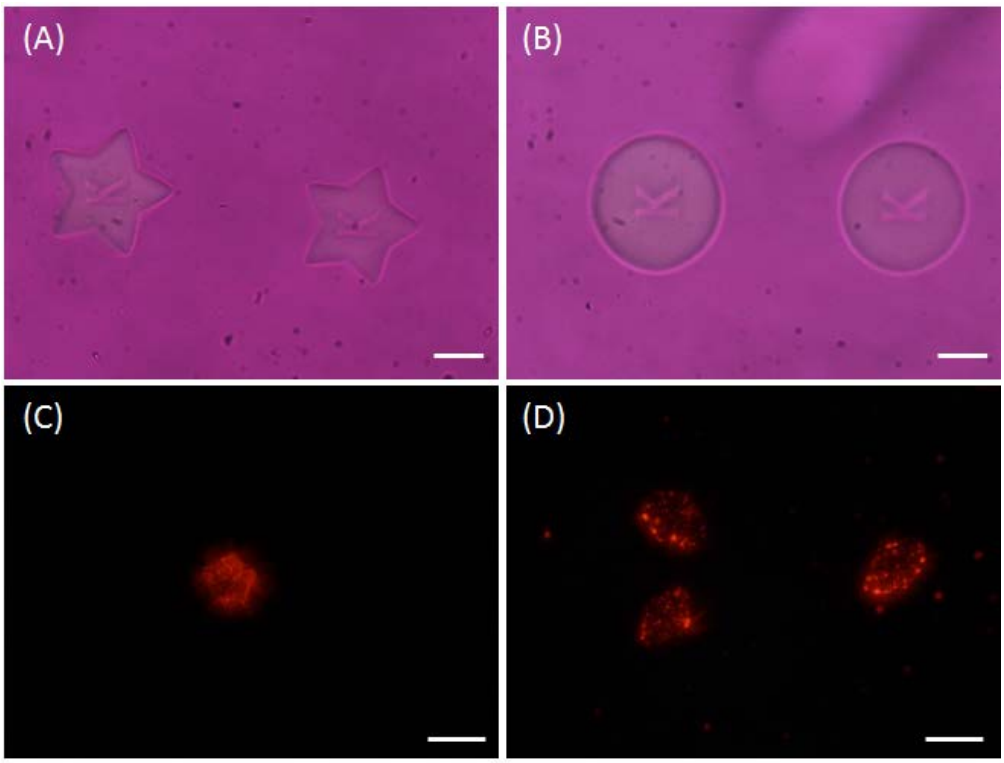

Figure 2.3 Images of shape-coded microparticles of small sizes. (A) Bright field image of star-shaped particles with the character “K”. The background appeared purple in color because the uncured polymer resin which contained rhodamine B had not been washed. (B) Bright field image of circle-shaped particles with character “K”. (C) Fluorescence image of pentagon-shaped particle (D) Fluorescence image of diamond-shaped particles. Fluorescence emissions of (C)-(D) were not uniform because the red fluorescent dye received from KOMSCO was not soluble in PEG-DA. (Scale bars: 50㎛)

Pentagon and diamond shaped microparticles were also fabricated with different fluorescent dye received from KOMSCO (Figure 2.3(C) and (D)). There were two problems with these particles. One was that fluorescence emissions from the particles were not uniform due to the property of the fluorescent dye. It was not soluble in the PEG-DA solution, unlike rhodamine B, so undissolved fluorescence molecules in the image appeared as dots. The other problem was that it was difficult to insert a character inside the particle because of the resolution limitation of the lithography system. Therefore, these fluorescence images of low resolutions might result in decoding problems.

In the second method, I synthesized larger particles than those shown above in order to facilitate both encoding of more letters inside the particles and detecting the code. Unlike small particles under 200㎛, it was difficult to fabricate large quantities of 500㎛ particles using the OFML system. In order to increase throughput, I tried to utilize photolithography with a film combine glass (FCG) mask. Circular and square particles encoded with the characters “BOK” were fabricated as shown in Figure 2.4(A) and (B). Compared to the smaller particles, the outer shapes and characters were more clearly visible under the microscope.

When the particle’s size became larger, however, it was easily folded and torn inside the solution because not only was the material of the particle soft polymer (PEG-DA), but the thickness of the particle was also much thinner than its width

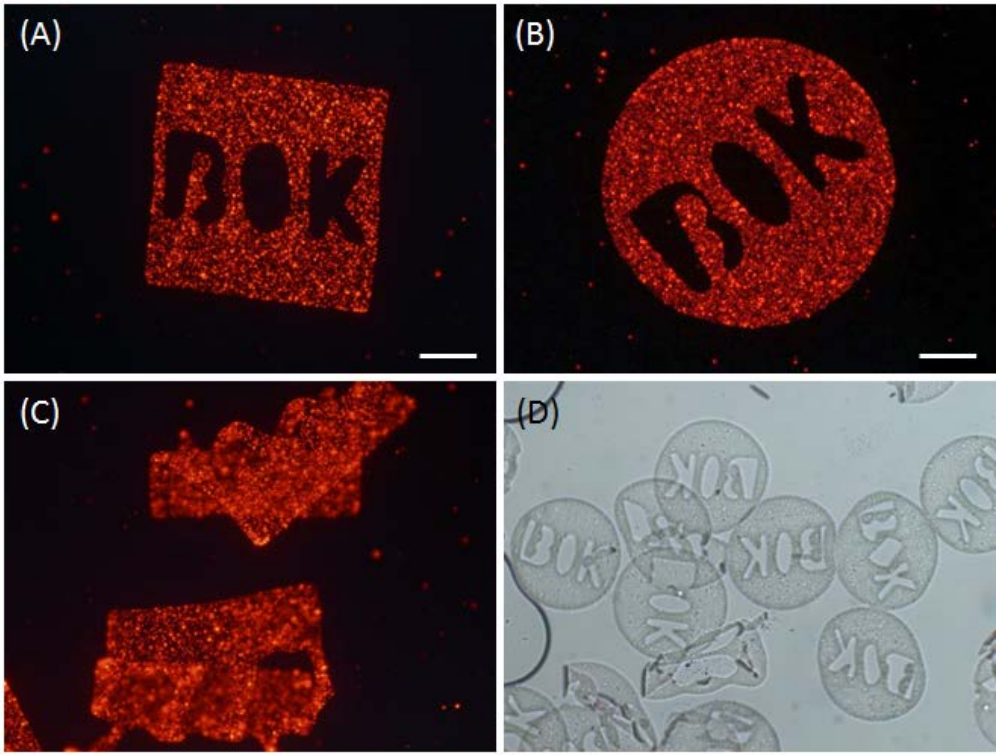

Figure 2.4 Images of synthesized shape-coded microparticles of large size. Fluorescence images show that more characters are encoded inside the particle with better resolution than in the particles of smaller sizes. (A) Square-shaped microparticle. (B) Circle-shaped microparticle (C) Folding of fabricated microparticles. (D) Tearing of microparticles. (C)-(D) shows that polymer particles that experience physical stress have problems of such as folding and tearing because they are made from a soft polymer and are very thin. (Scale bars: 100㎛)

(Figure 2.4(C) and (D)). The thickness of the particles was 25㎛ because according to the corporation they should be less than 40㎛ thick in order to implant in paper substrates. Since microparticles will be mixed with the paper pulp during the stirring process, they must be durable in order to be integrated into the paper.

Also, particles made from PEG-DA shrink or swell depending on the external solution environment, and thus can be unstable during the manufacturing process.

2.3 Silica-coated microparticles

To improve mechanical properties of the polymer microparticles, I coated the surface of the shape-coded microparticles with silica by using a modified version of the Stöber method [25]-[26]. The silica-coating process will be introduced first, followed by a description of the application of silica-coated microparticles for anti-counterfeiting.

A schematic view of the overall silica-coating process is shown in Figure 2.5. Shape-coded microparticles were synthesized using the OFML system. Prepolymer resin for particles consisted of ethoxylated trimethylopropane triacrylate (ETPTA), 3-(trimethoxysilyl) propyl acrylate (TMSPA), and a photoinitiator. TMSPA provided functional groups for both the polymerization with ETPTA and the silica-coating. Fabricated particles were collected into the vial. Then an aqueous solution for silica-coating (a mixture of ethanol, deionized (DI) water, and ammonium hydroxide) was added to the vial. Finally, tetraethoxysilane (TEOS) was added and the vial was agitated in order to produce the reaction. As time passed, silica nanoparticles grew on the surface of the polymer particles through the reactions of hydrolysis and condensation. At the beginning of the coating process, silica-nanoparticles were

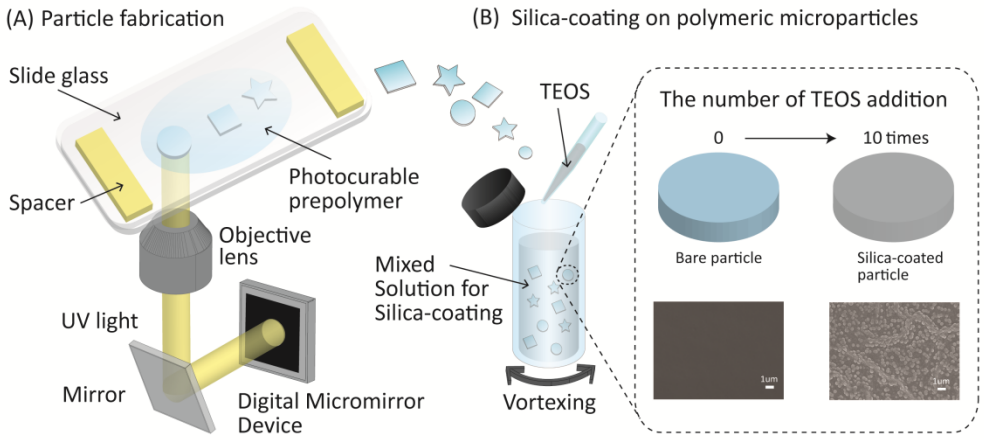

Figure 2.5 A schematic view of the silica-coating process. (A) Particle fabrication by photolighography (B) Silica-coating process. Scanning electron microscope (SEM) images inside the box show that silica nanoparticles were coated on the surface of fabricated polymeric particles as TEOS was added.

nucleated on the bare polymer surface. TEOS was added every 20 minutes and as time passed, silica-nanoparticles became more developed. After adding TEOS 10 times, they finally formed a silica layer that covered the entire surface of the particle (Figure 2.5(B)).

The characteristics of the fabricated silica-coated particles were tested depending upon the thickness of the particle. As shown in Figure 2.6, I chose 15㎛ and 40㎛ as thicknesses because these were the desirable minimum and maximum values able to be incorporated in papers. In both cases, the particles were successfully inserted inside the paper without severely damaging the particles because the hard silica layer on the surface enhanced the mechanical properties of

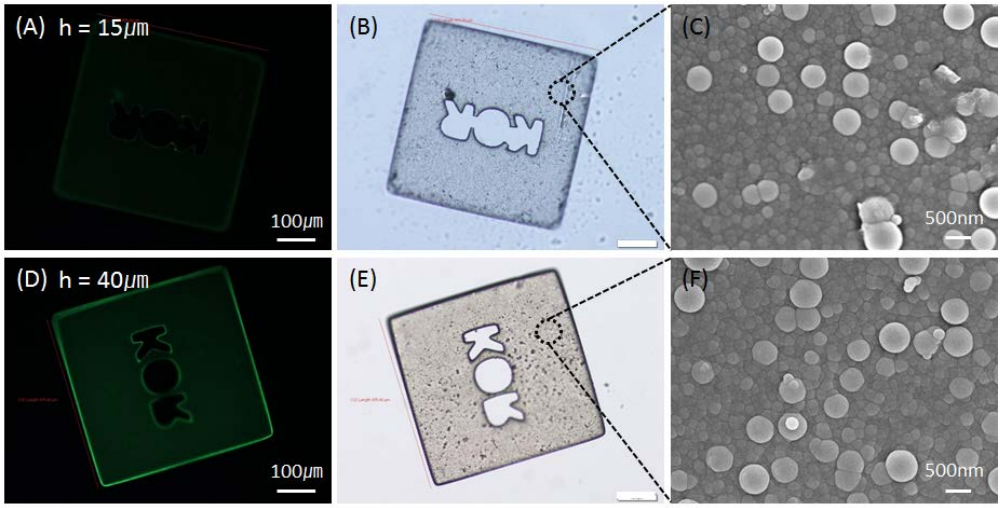

Figure 2.6 Images of silica-coated microparticles of two different thicknesses. (A) A fluorescence image of a 15㎛-thick particle. (B) A bright field image of (A). (C) A magnified SEM image of the particle surface. Silica nanoparticles covered the entire surface of the particle. (D) A fluorescence image of a 40㎛-thick particle. Fluorescence intensity was stronger than (A). (E) A bright field image of (D). (F) A magnified SEM image.

the particles. Resulting images of the microparticles integrated with the paper were not included in this thesis at the request of KOMSCO. As shown in the SEM images in Figure 2.6(C) and (F), silica-nanoparticles formed a silica layer on the surface of the particles. The silica-coating not only allowed microparticles to have enhanced mechanical properties, but also provided convenient storage capability when particles were dried.

Green fluorescent dye was used because green emissions were more clearly distinguishable than red fluorescence emissions under the illumination of UV light

on the paper. However, the fluorescence intensity was different depending on the thickness of the particle; the intensity was proportional to the thickness (Figure 2.6(A) and (D)). Therefore, it will be difficult to detect the fluorescence if the particle is very thin, making the selection of the appropriate thickness of particles important in the application to real banknotes.

The effect of particle's size was also tested (Figure 2.7). Four sizes of silica-coated particles (100, 200, 300, and 400㎛) with 25㎛–thick were fabricated and all were successfully incorporated into papers. In the size variation, the difference of the fluorescence intensity was less than in the thickness variation. However, the dimensions of the internal structures of the particles required careful design if the polymeric particles were to be silica-coated. When the empty region within the character borders was too close, this region was blocked by silica nanoparticles after the silica-coating process. Therefore, the size and the number of characters encoded on each particle are limited in smaller particles. Appropriate particle sizes can be selected by producers based on their specific needs regarding encoding shapes.

In this section, various sizes of shape-coded microparticles were fabricated and applied as a new tool for anti-counterfeiting of banknotes. To reduce damages to thin polymeric microparticles while they were being mixed with the paper pulp or inks, surfaces were coated with silica to make them harder, thereby facilitating the manufacture of papers with fabricated microparticles. The results demonstrated the

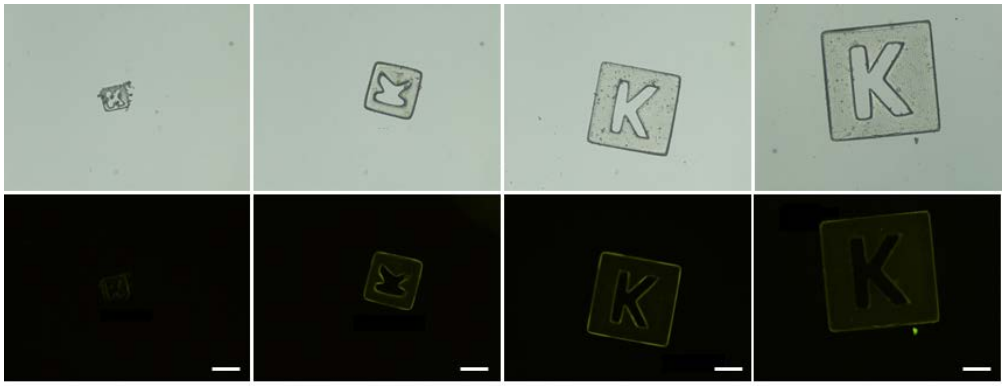

Figure 2.7 Bright field and fluorescence images of silica-coated microparticles of various sizes. Fluorescence images showed little difference of intensity according to the size. Enough space between the border lines within each character was needed to prevent blockage of the code by silica nanoparticles, especially in smaller particles. (Scale bars: 100㎛)

applicability of proposed microparticles coded by both shape and fluorescence as a new anti-counterfeiting method. Combined with techniques which are currently utilized for banknotes, this method could provide an even higher-level of security.

Chapter 3

QR-coded microparticles for anti-counterfeiting of drugs

In Chapter 3, another application of encoded microparticles is demonstrated using the QR-coded polymer microtaggant that provides high-capacity and error-correctable encoding for anti-counterfeiting of drugs.

3.1 QR code as a microtaggant coding scheme

The utilization of microtaggants, one ODA method, has received a lot of attention in the medicine industry as the amount of counterfeit drugs in the global pharmaceutical market continues to grow. Microtaggants carry information about drugs and are included inside each tablet or capsule during the manufacturing process in order to authenticate the drug. Such microtaggants are valuable in that it is difficult to detect and forge such tiny particles. When authentication techniques

are applied only in the packaging, the product inside cannot be protected because the changing of the inner contents and repackaging are quite easy. For instance, out-of-date or inappropriate materials could be substituted at some point during the distribution process. In this regard, microtaggants within a drug itself provide a very powerful and simple tool for preventing replication of drugs.

In order to authenticate drugs definitively, a lot of information should be encoded inside the microtaggants; product data such as ingredients, date of production, and expiration date, manufacturing data such as company name and lot number, and distribution data such as distributors and wholesalers. Therefore, coding schemes inside the microtaggants are required to have high data capacities so they are able to encode all of the above information. However, coding methods utilized in previous research may be insufficient for a large data capacity because they only coded one-dimensional (1D) barcodes or printed letters on the microtaggants using photobleaching of the fluorescence [16]-[18].

Although microtaggants retain a lot of data about the drug, they are useless if the encoded data is lost because of damage. For example, the microtaggants can be damaged by physical force during the tablet or capsule formulation processes of mixing, compressing, or packaging. Therefore an error correction function is required to decode data from the damaged microparticles so that pharmaceutical companies can not only guarantee the quality and safety of their products to

consumers, but also maintain their brand value.

To overcome these limitations and develop a high-level authentication method, QR code was selected as a new coding scheme for microtaggants. QR code is a type of two-dimensional (2D) matrix barcode, which consists of black square dots [27]-[31]. It provides higher data capacity than 1D barcodes in small areas. Also, due to the error correction algorithm of QR code, a partially damaged code can be recovered. In addition, specific position recognition patterns within QR codes allow omnidirectional reading without in-plane directional alignment, providing high-speed decoding.

3.2 Encoding QR-coded microparticles

Polymer microparticles patterned with QR codes were fabricated as shown in Figure 3.1(A). PEG-DA (Mn=700) with 10 wt% of a photoinitiator was used as the photocurable prepolymer solution. For fluorescent labeling, 1 mM methacryloxyethyl thiocarbamoyl rhodamine B was mixed with the PEG-DA solution. In order to generate the QR code pattern, QR code generating software was used from an open source library [32].

As shown in Figure 3.1(B), QR code consists of the data area and position detection patterns. The position detection patterns are the same as each other and exist in a fixed area found in three corners of each code. However, data patterns are

randomly generated as a 2D array of unit modules depending on the encoded information. In order to decode QR code, this array of unit modules should be patterned using high resolution on the polymer microparticles. QR code patterns inside the fabricated particle showed good resolution similar to the original mask pattern as shown in Figure 3.1(A).

QR code was patterned lithographically on the polymeric microparticles using the OFML system (Figure 3.1(C)). UV light from the UV source was patterned as QR code shapes through the DMD pattern. In this step, the mask image of QR code for DMD should be a horizontally flipped version of the original image in order to correctly pattern the code on the microparticle. Patterned UV light was projected onto the microfluidic channel and QR-coded microparticles were synthesized by photopolymerization of polymer resin through a single exposure.

As shown in Figure 3.1(D), a fluorescent acrylic monomer was used to enhance the contrast of the QR code image so that the code pattern could be clearly distinguishable from the background with the use of a digital detector. Since this acrylic dye was polymerized with PEG-DA, it did not leak from the particle substrate to the external solution. Therefore fluorescence could be stably maintained for a long time. The line profile of the fluorescence intensity showed that the ratio of the low to the high intensity level was approximately 0.35, which was sufficient to provide a clear on/off threshold value for reading the code. The code in the image

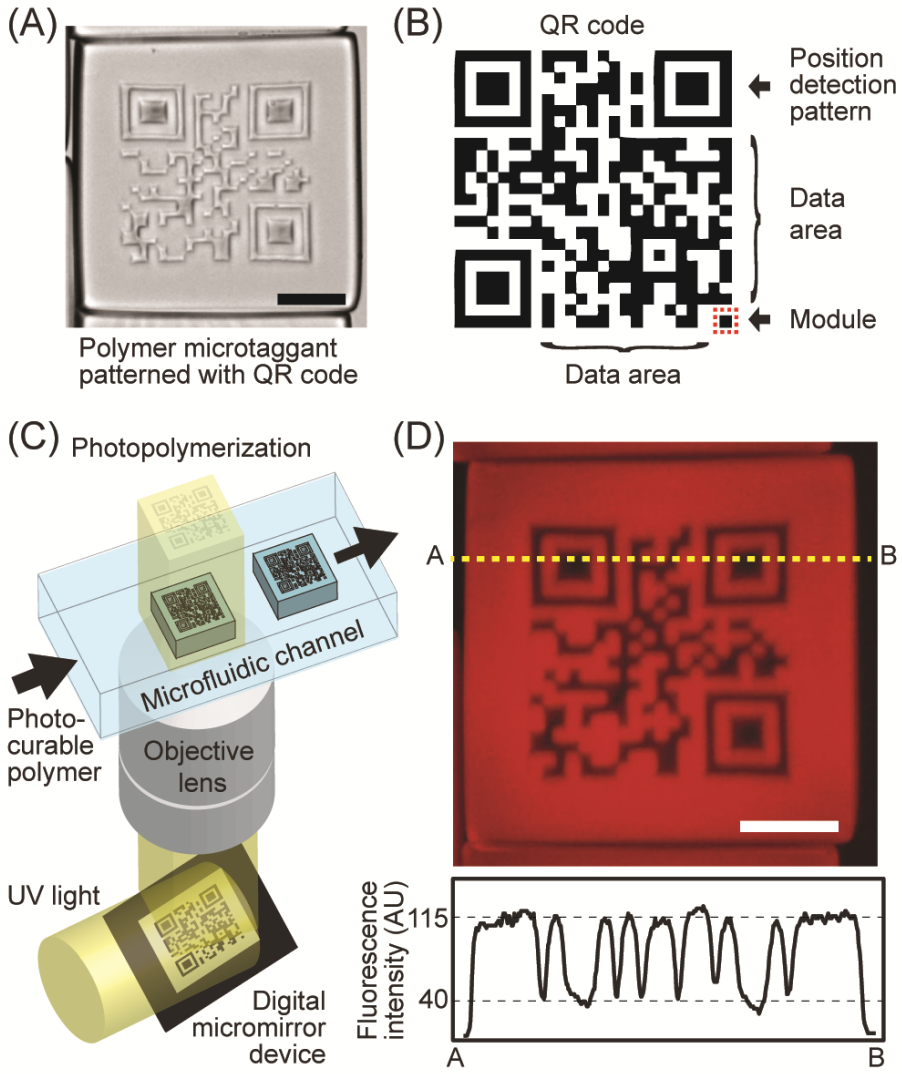

Figure 3.1 Fabrication of QR-coded microtaggants (A) Microscope image of polymer microtaggant patterned with QR code (Scale bar: 200㎛) (B) The structure of a QR code. Position detection patterns, large and square in shape, are located at three corners of the code, which allow detection of the edges of the code. Data area consists of unit modules comprised of black square dots. (C) The OFML system for the fabrication of QR-coded microparticles (D) Fluorescence microscopic image of the QR-coded microtaggant and the line profile (A-B) of the fluorescence intensity (Scale bar: 100㎛) [19].

was decoded correctly using a common smartphone application for reading QR code.

Since the QR code mask is a combination of small white and black dots, white dots can be isolated by black outer dots. A lot of such island patterns exist in the QR code; for examples, the big square rings in the position detection pattern and the arbitrary shapes of the white dots in the coding region. This island pattern does not matter when the QR code is printed on substrates such as paper. However, it does matter when QR code is lithographically patterned as a free-floating structure without a substrate because the isolated region can be separated from the body. To prevent this problem, experiment parameters were designed based on an investigation of the 3D UV propagation characteristics inside a microfluidic channel.

In the OFML system, projected UV light enters perpendicular to the bottom of the microfluidic channel and propagates along the *z*-direction. Let's assume that focal plane is at the bottom of the channel. As the light propagates from the focal plane, it spreads horizontally (Figure 3.2). Therefore, UV rays, separated by black modules on the DMD mask through which light cannot pass, overlap far from the image plane [33]. If the vertical position of the light overlap plane is over the top of the channel, island patterns are separated from the microtaggant. On the contrary, if the vertical position of the light overlap plane is below the top of the channel and the UV intensity in the overlap plane is strong enough to initiate polymerization of PEG-DA, island patterns are connected to the neighboring part by the

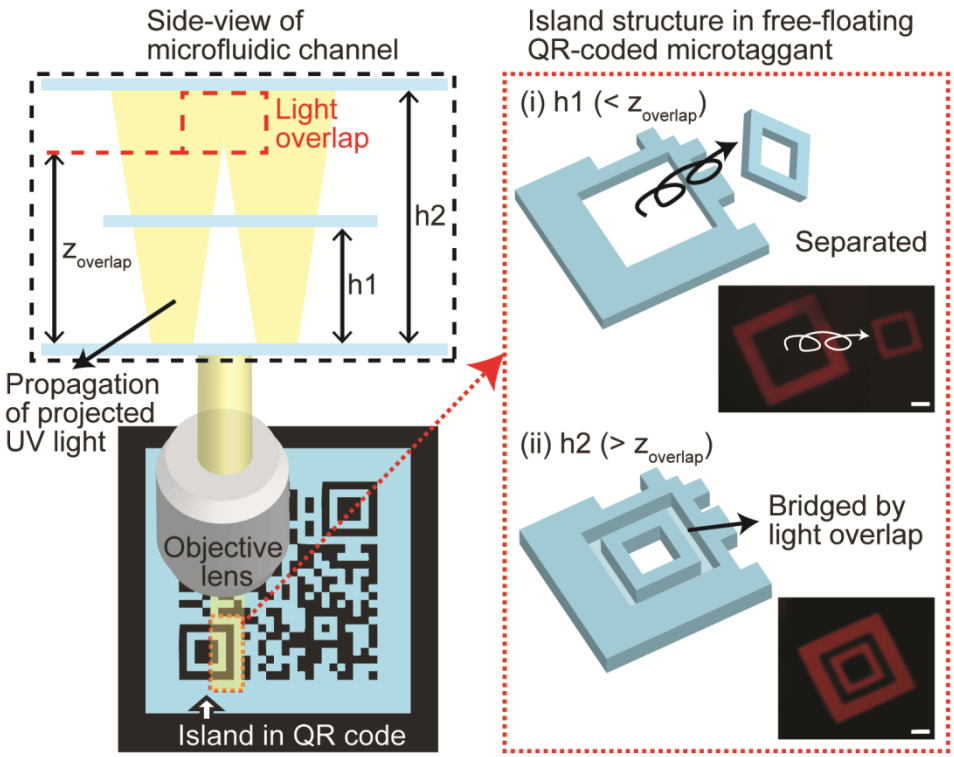

Figure 3.2 Fabrication of free-floating QR-coded microtaggants without separation of island structures. The left schematic shows propagation of patterned UV light projected through a QR code mask along the *z*-axis inside the microfluidic channel. (i) When the channel height (h1) was lower than the light overlap position ($Z_{overlap}$), the island structure was separated from the microparticle. (ii) When the channel height (h2) was higher than $Z_{overlap}$, the island structure remained inside the microtaggant (Scale bars: 40㎛) [19].

polymerization of PEG-DA in the light overlap area. Therefore, the propagation characteristics of the projected UV light and the height of the microfluidic channels are crucial parameters for the connection of the island structure. The propagation characteristics mainly depend on both the module size of the QR code and the

energy distribution of the projected UV light.

Propagation characteristics of the projected UV light were simulated using the scalar diffraction theory to find light overlap region inside the microfluidic channel according to the module sizes [34]. UV light was assumed to be normally incident, incoherent, and polychromatic with a narrow-band wavelength distribution, to form an image intensity distribution in (x, y) plane at various beam propagation distances. The projection lens was assumed to have a square lens aperture with a diagonal length of 8.1mm, a numerical aperture of 0.3, and a focal length of 13.5mm. Under the assumption of paraxial ray considerations, the light intensity distribution near the image plane can be approximately described as

$$I_i(x,y,z) = |h(x,y,z)|^2 \otimes I_g(x,y), \qquad z = z_i + \Delta z \tag{3.1}$$

$$h(x,y,z) = \frac{1}{\lambda^2 z_0 z}\iint P(\xi,\eta) exp\left[j\frac{\pi}{\lambda}\left(\frac{1}{z_0}+\frac{1}{z}-\frac{1}{f}\right)(\xi^2+\eta^2)\right] exp\left[-j\frac{2\pi}{\lambda z}(x\xi+y\eta)\right] d\xi d\eta \tag{3.2}$$

where I_g is the intensity distribution of an ideal image, $\otimes$ is the convolution integral, z is the propagation distance from the projection lens, z_i is the propagation distance from the image plane, Δz is the deviation from the image plane along the z-axis, z_0 is the distance between a mask and the projection lens, λ is a light wavelength, P is a pupil function in (ξ, η) plane, and f is a focal length of the projection lens [33].

With the specific height of the channel assumed, the module size should be controlled to prevent separation of island structures. Simulation parameters and

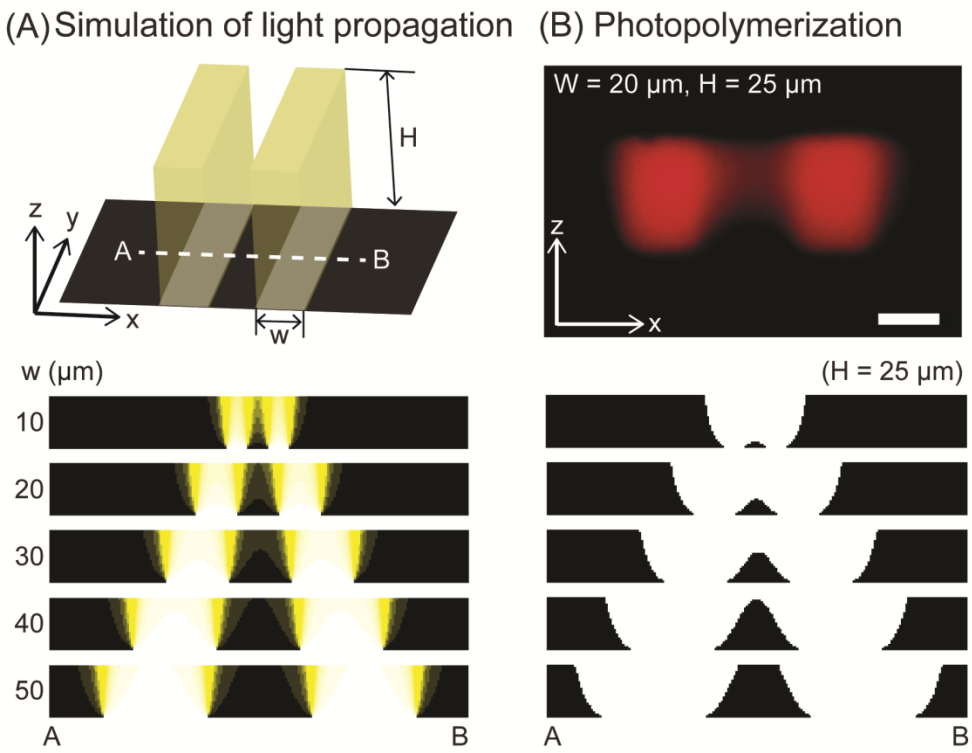

Figure 3.3 Analysis of propagation and intensity distribution of the projected UV light across the *x*-*z* plane in the microfluidic channel (A) Distribution of light intensity with regard to various module widths. Two parallel lines represent two neighboring modules. The width of the lines (w) and the distance between them were set to be identical, and the height of the channel was fixed at 25㎛. (B) The expected shape of polymerization inside the microchannel depended on the module width. The threshold value for the initiation of photopolymerization was derived from experimental observation. Using light with intensity greater than the threshold value, expected polymerized structures were derived. When the width was larger than 40㎛**,** two patterns were separated (Scale bar: 20㎛) [19].

conditions are shown in Figure 3.3(A). Two lines parallel to the *y*-axis (corresponding to the two neighboring modules) represent a projected UV light

pattern. The width of the two lines (w) and the distance between them (representing the module size of QR code) were set to be identical. The height of the channel was fixed at 25㎛. The light intensity distribution of this pattern across the *x*-*z* plane was calculated with respect to different module widths: 10, 20, 30, 40, and 50㎛. The shape of the polymerized structure was drawn from the calculated light intensity distribution by applying a specific threshold (Figure 3.3(B)). This threshold value was derived based on the experimental result, shown in the fluorescence image in Figure 3.3(B). Separation of the two structures occurred when the module width was larger than 40㎛ in the channel. Therefore, all QR-coded microtaggants used in this research were fabricated in channels with heights greater than 25㎛ and with code masks with module widths of less than 40㎛.

The maximum data capacity of a QR code is determined by its symbol version. The symbol version of QR codes range from 1 to 40, and each version has a different number of modules. More modules are required to encode more data. In addition, data capacity also depends on the error correction level and the character type. Four levels of error correction can be selected. Higher error correction levels allow for the recovery of more data from the damaged area, but data capacity decreases as the error correction level increases. More than twice the total amount of data can be encoded using the lowest error correction level as opposed to using the highest level in the same QR code version. Also, various types of data can be

utilized within QR codes: numeric only, alphanumeric, binary, and other languages including the control code. Each type provides different data capacities even in the same version.

To demonstrate high capacity encoding on the QR-coded microtaggant, four different versions (1, 4, 7, and 10) were selected and fabricated using the maximum error correction level (Figure 3.4). Also, an alphanumeric data type was selected because it was the most appropriate form for providing drug information such as the product name, production data, expiration data, manufacturer, and webpage links. Each version of QR code had different numbers of modules. The fabricated four versions consisted of 21, 33, 45, and 57 modules for each row and column. Each version encoded 10, 50, 93, and 174 characters, respectively. This capacity corresponds to 56, 272, 512, and 952 bits as binary type. Although data capacity increased at the cost of the data recovery rate, the highest error correction level was selected here because error correction capacity, in addition to data capacity, was regarded as an important function for the microtaggant. For encoding of drug information, it was thought that a symbol version of higher than 7 with the maximum error correction level would be sufficient.

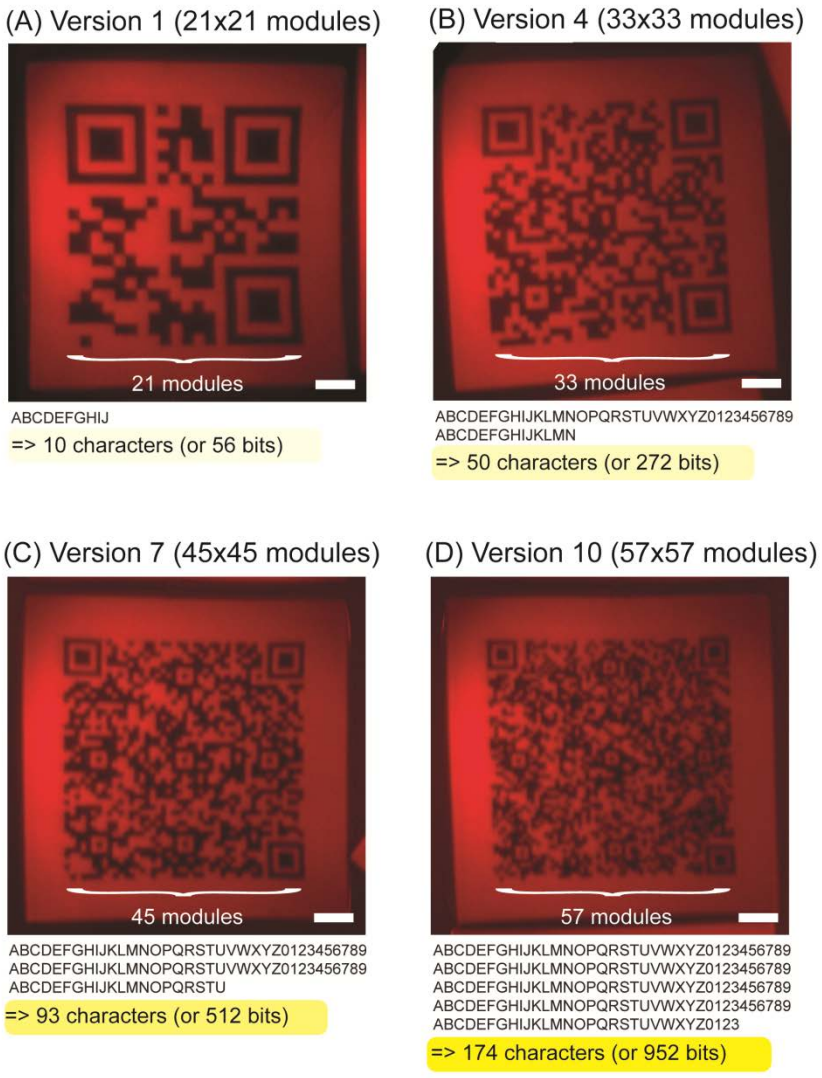

Figure 3.4 Encoding capacity of QR-coded microtaggants. The data capacity is determined by the symbol version, error correction level, and data type of the QR code. Four types of versions (1, 4, 7, and 10) were applied to show the data encoding capacity. In this demonstration, the maximum error correction level was selected and an alphanumeric data type was used. (A) Version 1. 10 characters were encoded. (B) Version 4. 50 characters were encoded. (C) Version 7. 93 characters were encoded. (D) Version 10. 174 characters were encoded (Scale bar: 50㎛) [19].

3.3 Decoding QR-coded microparticles

Fabricated QR-coded microparticles were detected using a true-color charge-coupled device (CCD) camera (DP72, Olympus) equipped with an optical microscope (IX 71, Olympus). Acquired QR code microscopic images were decoded using a QR code reader application (QuickMark, SimpleAct, Inc.) on a smartphone (Galaxy S, Samsung Electronics Inc. or iPhone 4, Apple Inc.). Error correction capability and demonstration of the authentication process of a drug will be discussed here.

Error correction capability is one of the distinguishing features of the QR code. Four error correction levels (L, M, Q, and H) are available in the QR code. The levels restore data of approximately 7%, 15%, 20%, and 30%, respectively, from the damaged code. Level Q and H may be selected in an environment where damages of microtaggants might occur, such as in manufacturing factories, and level L and M would be appropriate in a relatively clean environment.

In order to investigate how the error correction capability of QR code provides damage resistance to the microtaggant, we intentionally damaged QR-coded microtaggants and then read them (Figure 3.5). At level L, the data encoded on the particle having a scratched area of less than 5% of the data region was successfully recovered. However, the particle, with a missing area of more than 30% located in the middle region of the code, was not able to be decoded (Figure 3.5(A)). At level H, approximately 20% damage to the data area did not affect recovery of the data.

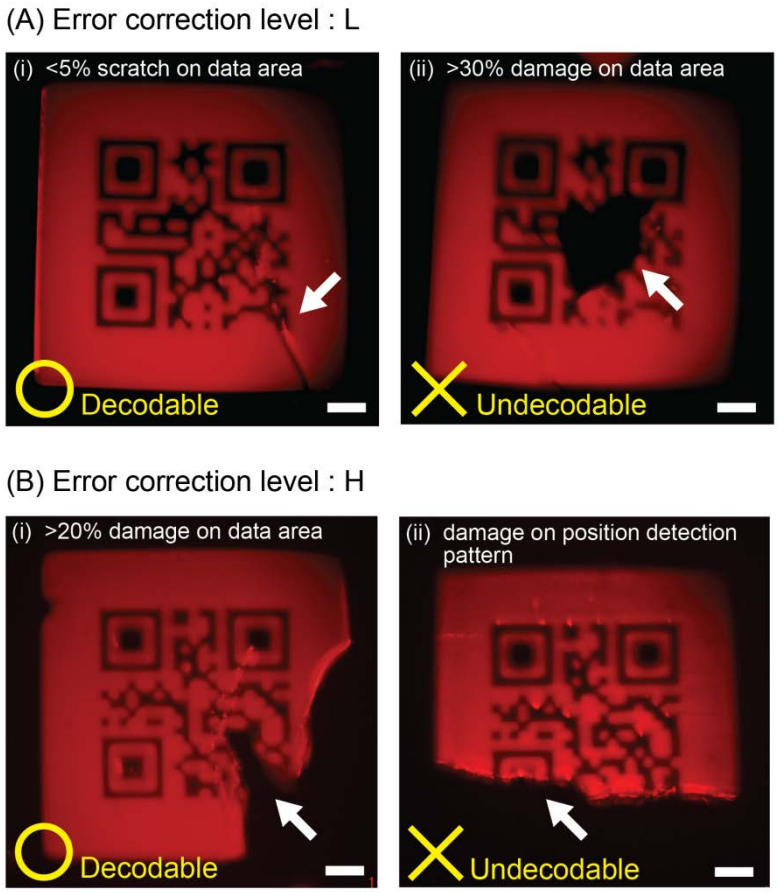

Figure 3.5 Error correction capability of microtaggants from damages. Four error correction levels (L, M, Q, H) are available, which can restore data up to 7%, 15%, 20%, and 30%, respectively. (A) Microtaggants coded by level L. The code having damage amounting to less than 5% of the data area was restored, although the code having damage of more than 30% was not. (B) Microtaggants coded by level H. Damage to approximately 20% of the data area was decoded, whereas damage to the position detection pattern was not regardless of the degree of damage (Scale bar: 50 ㎛) [19].

However, the code having damage on the position detection pattern was not able to

be decoded, even at the H level (Figure 3.5(B)). The capability of data recovery from codes with physical damages give microtaggants a powerful advantage, due to the high possibility of physical damage when they are incorporated into the capsule or tablet during the formulation process.

QR code also features omnidirectional reading capability through position detection patterns located at three corners of the code. Since QR code is readable from any direction, QR-coded microparticles can be decoded without alignment between the microtaggant and the code reader device, allowing high-speed authentication. As shown in Figure 3.6, microtaggants of different angles were correctly decoded. Since various decoding software of QR codes have been developed on the smartphone platform, QR-coded microtaggants can be easily applicable as an ODA method by just utilizing a conventionally available QR code software, thus saving time and reducing costs compared to the construction of advanced ODA platforms.

To verify the applicability of QR-coded microtaggants to medicine, I formulated a drug capsule with the microtaggants, encoding some drug information, and then demonstrated the authentication process. First, the microtaggants inside the capsule were detected using a microscope after opening the capsule (Figure 3.7(A)). Under this condition, QR code could not be decoded because of the drug powder near the microtaggants as shown in Figure 3.7(B). Therefore, in the next step, the

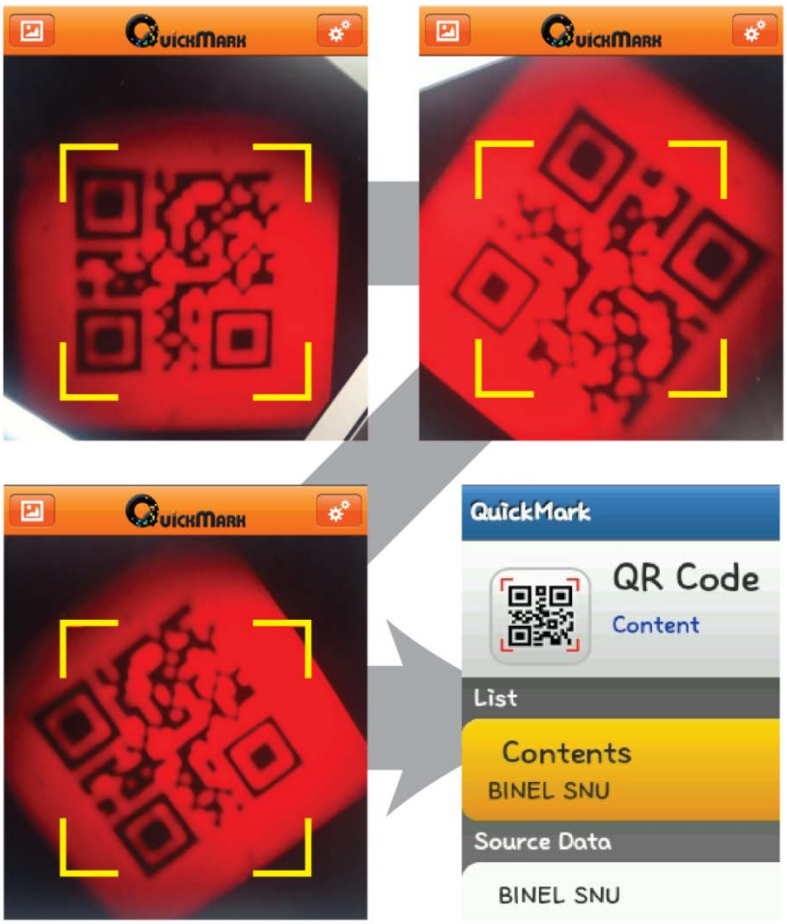

Figure 3.6 Demonstration of omnidirectional reading of QR-coded microtaggants. The QR code on microparticles was successfully decoded regardless of their position relative to a code reader device. Microtaggants were read by a smartphone with the QR code application software. All images were captured from the smartphone screen [19].

drug powder was dissolved and washed off in pure water, and then a clear fluorescence image was obtained (Figure 3.7(C)). Finally, the obtained image of the QR-coded microtaggant was successfully decoded by reading it using the QR code

reader application of a smartphone (Figure 3.7(D)). Since the drug information such as the product name, production data, expiration data, and website link are displayed on a smartphone, users can authenticate the drug using this process

Although use of QR-coded microtaggants is proposed to prevent counterfeiting of drugs, counterfeiting of the microtaggant itself is possible by someone who has a photolithography system that can synthesize microparticles. In this case, authentication capability could be improved by combining raw materials such as DNA and optical materials with spectral signatures.

Fabricated QR-coded microparticles should be safe inside the human body because they are ingested with drugs. PEG-DA, the major component of the particle, has been widely used in various studies related to tissue engineering, transplantation, and drug delivery [35]-[37]. However, the fluorescence dye may be toxic to the body. In this research, the fluorescent acrylic monomer was used to completely copolymerize it with PEG-DA. Therefore, diffusion of fluorescent molecules was minimized after synthesizing the microtaggants. Also, in this experiment, each QR-coded microparticle contained approximately 20 ng of fluorescent dye, as the concentration of it in an oligomer mixture was 1mM. If we assume that a tablet contains ten microtaggants and a patient takes three capsules a day, he/she takes approximately 220 μg of fluorescent dye in a year and this level is considerably lower than the LD50 (887 mg kg^{-1} in a mouse) [38].

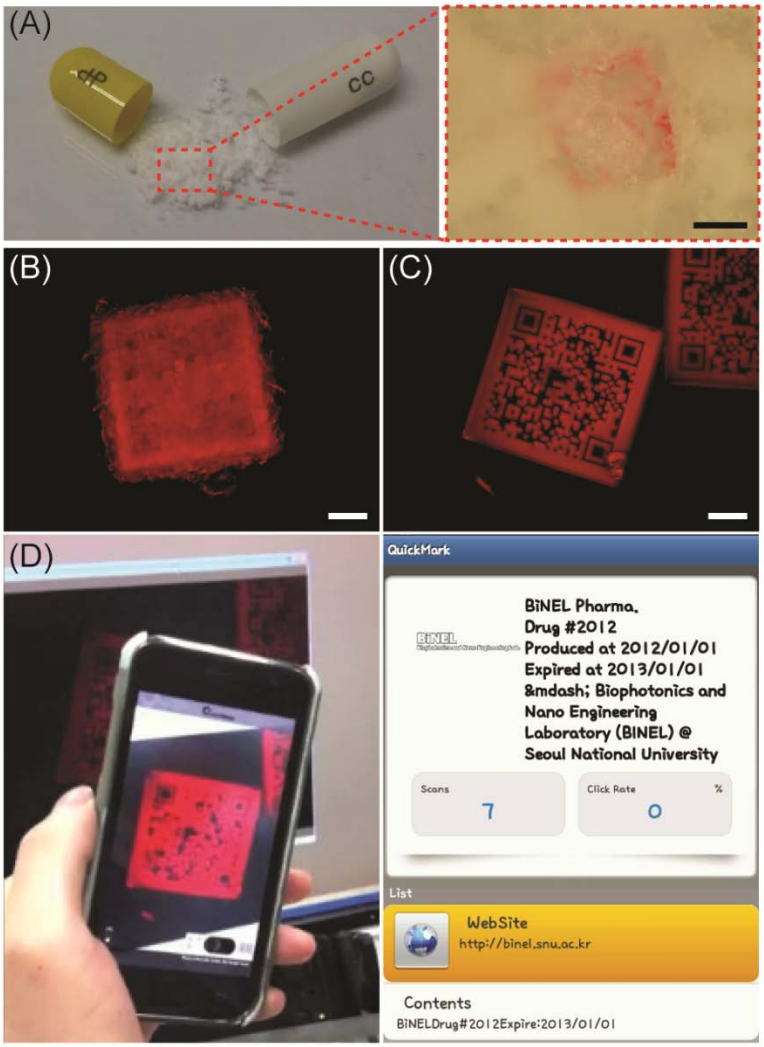

Figure 3.7 Authentication process for the anti-counterfeiting of a drug using QR-coded microtaggants (A) A fabricated drug capsule containing the microparticles. First, a capsule was opened and microtaggants were detected using a microscope. (Scale bar: 200㎛) (B) A fluorescence image of the microtaggant before washing. Second, a drug powder was dissolved in water in order to read the code. (C) A fluorescence image after washing. (Scale bars: 100㎛) (D) Decoding of the drug information. Finally, the microscopic image of the microtaggant was read using a QR code reader application on a smartphone. The drug was successfully authenticated [19].

In addition, to verify the toxicity of the microtaggants to cells, the cell viability assay was conducted using cells cultured with microtaggants. QR-coded microtaggants were fabricated with four different concentrations of the photoinitiator, washed with ethanol, and dried overnight in a clean bench with UV illumination. Two kinds of cell lines were used for the cytotoxicity tests: porcine stable (PS) kidney cells and U2OS cells. After cells were prepared in the 96-well plate, the dried microtaggants were added into cells at the ratio of 1.2×10^3 and 13.8×10^3 cells per microtaggant, respectively. The cells were incubated with QR-coded microtaggants overnight and cell viability was measured. As shown in Figure 3.8, more than 95% of the cells survived in all concentrations of the photoinitiator, which confirmed that the proposed QR-coded microtaggants are non-cytotoxic.

In the proposed authentication process, a conventional microscope was used to get images of microparticles, although code decoding was conducted on a smartphone. To facilitate the imaging process, I tried to read the microtaggant using a portable microscope that is a commercially available device (usbfever Ltd.) (Figure 3.9(A)). Since this device is compatible with the iPhone, users can take a picture of the QR code on the microtaggant just by attaching the device to the smartphone and running the camera software on the smartphone. Then the pictured image can be loaded and decoded by the QR code application. Although this process was much more convenient than the previous process, I did not succeed in decoding

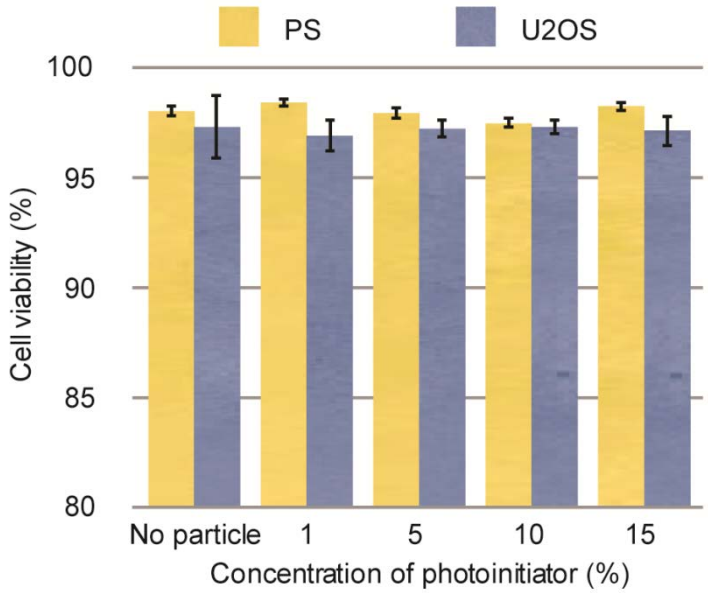

Figure 3.8 Cytotoxicity tests of QR-coded microtaggants with respect to four different concentrations of the photoinitiator. The cell viability assay was conducted after culturing porcine stable (PS) and U2OS cells with dried QR-coded microtaggants. No significant drop of cell viability was observed in all conditions compared to the control [19].

the code because the resolution of images taken from the device were not good enough to be decoded. In order to use the portable device, other techniques such as image processing, should be included to increase imaging resolution.

In addition, QR-coded microtaggants were synthesized using various food dyes, in addition to the fluorescent dye, in order to enhance color contrast between the background and the code even in bright field images (Figure 3.9(B)). The code was successfully decoded on the bright field image of a conventional microscope (Figure 3.9(C)-(D)), but the code was not able to be decoded on the image of the portable

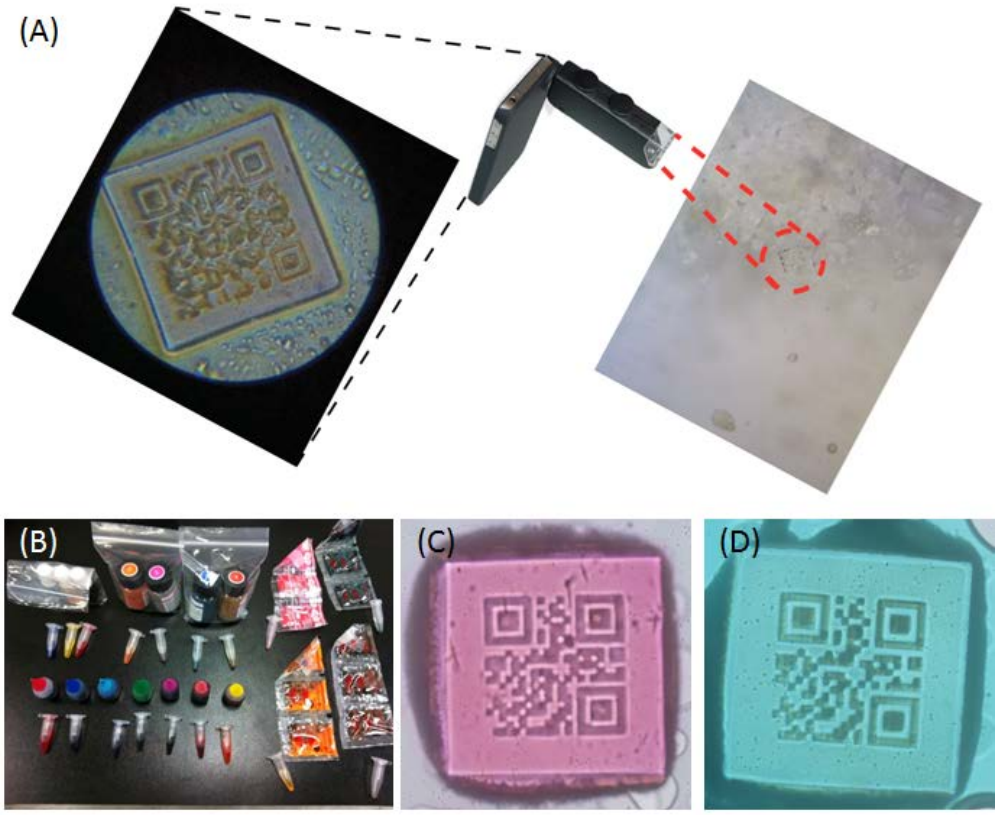

Figure 3.9 Code decoding using a portable microscope and fabrication of QR-coded microtaggants with food dyes (A) An image pictured from the portable microscope. Although the portable microscope facilitated reading of the taggant, the pictured image was not able to be decoded by the smartphone application because the image resolution was not good. (B) Various food dyes used for particle fabrication (C) A bright field image of a microtaggant dyed red (D) A microtaggant dyed blue. (C)-(D) were photographed using a conventional microscope and were successfully decoded.

microscope. Food dye taggants can be utilized as a substitute for fluorescent dye taggants if patients are unwilling to ingest the fluorescent dye.

In this section, I proposed QR-coded microparticles for anti-counterfeiting of drugs. Fabricated microtaggants featured high encoding capacities, error correction capabilities, and omnidirectional reading capabilities. The authentication process was demonstrated using a drug capsule containing QR-coded microtaggants encoded with drug information. Cell viability for the fabricated microtaggants was tested to verify the safety of the proposed ODA method. Also, the feasibility of using a portable microscope in the reading process was tested, but the result was unsuccessful. In addition, it was demonstrated that food dyes could be used as a substitute for the fluorescent dye.

Chapter 4

Conclusion

In conclusion, this thesis has presented encoded microparticles as a new tool for anti-counterfeiting techniques and has demonstrated its application possibilities for banknotes and drugs. In the first section, shape-coded microparticles were fabricated using fluorescent dyes for application to banknotes. Various codes were applied by changing both the shape (such as the outer shape, the inner character, and the size) and the fluorescent dye. By combining these two coding elements, the security level of a banknote can be increased and it becomes significantly more difficult for a criminal to forge the banknote. Fabricated microparticles were mixed with the paper pulp during the manufacturing process or mixed into the ink used for printing. Since polymer particles were vulnerable to physical damage during the manufacturing process, I coated the surface of the microparticles with silica to enhance mechanical

properties of the particles. Silica-coated microparticles were successfully integrated into the paper. During the final authentication process, verification began by checking for the existence of the microparticles using fluorescence imaging and then by decoding codes on each microparticle using a microscope. The research is in progress with KOMSCO and I expect that this new, particle-based anti-counterfeiting technology, can increase security complexity when it is combined with other conventional authentication technologies currently in use with banknotes. Also, shape-coded microparticles could prove to be a valuable anti-counterfeiting tool for other paper based materials in addition to banknotes.

In the second section, I presented QR-coded microparticles as an anti-counterfeiting tool for drugs. QR coding was selected as a coding scheme because it provided both high data capacity and the error correction function. The module size of the code and the height of the microfluidic channels were decided through the analysis of the UV light propagation in order to prevent the separation of island patterns. High encoding capacity, error correction, and omnidirectional reading ability were demonstrated using fabricated QR-coded microtaggants, and the authentication process was illustrated using a drug capsule containing QR-coded microtaggants. In addition, the toxicity of the fabricated microparticles was tested by a cell viability test, and the test verified that they were not cytotoxic. As another decoding approach, I photographed the QR codes on the microparticles using a

portable microscope instead of a conventional microscope, but decoding failed because the image quality was too low. In future research, use of image processing software would likely improve image quality and be valuable because drug authentication using QR-coded microtaggants would be greatly facilitated if users could use a portable microscope. Additionally, QR-coded microtaggants which included a food dye instead of a fluorescent dye were successfully decoded on the bright field image, thereby demonstrating how a food dye could possibly be a substitute for a fluorescent dye and might prove safer for patients.

Bibliography

[1] R. A. Lee, “ Micro-Technology for Anti-Counterfeiting, ” *Microelectronic Engineering*, vol. 53, pp. 513-516, 2000.

[2] P. W. Leech and R. A. Lee, “Hot embossing of diffractive optically variable images in biaxially-oriented polypropylene, ” *Microelectronic Engineering*, vol. 84, pp. 25-30, 2007.

[3] H. I. Bjelkhagen, *Optical and Digital Techniques for Information Security*. New York: Springer, 2005, chapter 2.

[4] P. W. Leech and H. Zeidler, “ Microrelief structures for anti-counterfeiting applications,” *Microelectronic Engineering*, vol. 65, pp. 439-446, 2003.

[5] S. Berthier, J. Boulenguez, and Z. Balint, “Multiscaled polarization effects in *Suneve coronate* (Lepidoptera) and other insects: application to anti-counterfeiting of banknotes,” *Applied Physics A*, vol. 86, pp. 123-130, 2007.

[6] Y. T. Lu and S. Chi, "Compact, reliable asymmetric optical configuration for cost-effective fabrication of multiplex dot matrix hologram in anti-counterfeiting applications," *Optik - International Journal for Light and Electron Optics*, vol. 114, pp. 161-167, 2003.

[7] R. W. Phillips and A. F. Bleikolm, "Optical coatings for document security," *Applied Optics*, vol. 35, pp. 5529-5534, 1996.

[8] S. Huang and J. K. Wu, "Optical Watermarking for Printed Document Authentication," *IEEE Transactions on International Forensics and Security*, vol. 2, pp. 164-173, 2007.

[9] G. S. Spagnolo, L. Cozzella, and C. Simonetti, "Banknote security using a biometric-like technique: a hylemetric approach," *Measurement Science and Technology*, vol. 21, 055501, 2010.

[10] U. Zschieschang, T. Yamamoto, K. Takimiya et al., "Organic Electronics on Banknotes," *Advanced Materials*, vol. 23, pp. 654-658, 2011.

[11] M. Schiek, F. Balzer, K. Al-Shamery et al., "Organic Molecular Nanotechnology," *Small*, vol. 4, pp. 176-181, 2008.

[12] R. Y. Shah, P. N. Prajapati, and Y. K. Agrawal, "Anticounterfeit packaging technologies," *Journal of Advanced Pharmaceutical Technology & Research*, vol. 1, pp. 368-373, 2010.

[13] P. M. O. Wong, "On-dose authentication: Walking softly, prepared to stick," *Tablets & Capsules*, vol. 9, pp. 28-33, 2011.

[14] U. S. Food and Drug Administration, Guidance for Industry: Incorporation of Physical-Chemical Identifiers into Solid Oral Dosage From Drug Products for Anticounterfeiting, 2011, *http://www.fda.gov/downloads/Drugs/GuidanceComplianceRegulatoryInformation/Guidances/UCM171575.pdf*

[15] F. Fayazpour, B. Lucas, N. Huyghebaert et al., "Digitally Encoded Drug Tablets to Combat Counterfeting," *Advanced Materials*, vol. 19, pp. 3854-3858, 2007.

[16] C. Huang, B. Lucas, C. Vervaet et al., "Unbreakable Codes in Electrospun Fibers: Digitally Encoded Polymers to Stop Medicine Counterfeiting," *Advanced Materials*, vol. 22, pp. 2657-2662, 2010.

[17] K. Braeckmans, S. C. D. Smedt, C. Roelant et al., "Encoding microcarriers by spatial selective photobleaching," *Nature Materials*, vol. 2, pp. 169-173, 2003.

[18] S. E. Chung, W. Park, H. Park, et al., "Optofluidic maskless lithography system for real-time synthesis of photopolymerized microstructures in microfluidic channels," *Applied Physics Letters*, vol. 91, 041106, 2007.

[19] S. Han, H. J. Bae, J. Kim et al., "Lithographically Encoded Polymer Microtaggant Using High-Capacity and Error-Correctable QR Code for Anti-Counterfeiting of Drugs," *Advanced Materials*, vol. 24, pp. 5924-5929, 2012.

[20] G. M. Whitesides, E. Ostuni, S. Takayama et al., "Soft Lithography in Biology and Biochemistry," *Annual Review of Biomedical Engineering*, vol. 3, pp. 335-373, 2001.

[21] D. Dendukuri, D. C. Pregibon, J. Collins et al., "Continuous-flow lithography for high-throughput microparticle synthesis," *Nature Materials*, vol. 5, pp. 365-369, 2006.

[22] D. Dendukuri, S. S. Gu, D. C. Pregibon et al., "Stop-flow lithography in a microfluidic device," *Lab on a Chip*, vol. 7, pp. 818-828, 2007.

[23] 한상권, 박 욱, 권성훈, "폴리머 마이크로 입자의 고속 생산을 위한 광미세유체 스텝 앤 리핏 마스크리스 리쏘그래피," *제13회 한국MEMS학술대회*, 89-90쪽, 2011년 4월.

[24] *http://www.merit.co.kr/merit/bbs/board.php?bo_table=oa4&wr_id=4*

[25] W. Stöber, A. Fink, and E. Bohn, "Controlled Growth of Monodisperse Silica Spheres in the Micron Size Range," *Journal of*

Colloid and Interface Science, vol. 26, pp. 62-69, 1968.

[26] J. Ge and Y. Yin, "Magnetically Tunable Colloidal Photonic Structures in Alkanol Solutions," *Advanced Materials*, vol. 20, pp. 3485-3491, 2008.

[27] H. Kato and K. T. Tan, "Pervasive 2D barcodes for camera phone applications," *IEEE Pervasive Computing*, vol. 6, pp. 76-85, 2007.

[28] E. Ohbuchi, H. Hanaizumi, and L. A. Hock, "Barcode readers using the camera device in mobile phones," in *Proc. of the 2004 International Conference on Cyberworlds*, Nov. 18-20, 2004, pp. 260-265.

[29] P. Premaratne and F. Safaei, "2D Barcodes as Watermarks in Image Authentication," in *Proc. of 6th IEEE/ACIS International Conference on Computer and Information Science*, Jul. 11-13, 2007, pp. 432-437.

[30] J. Z. Gao, L. Prakash, and R. Jagatesan, "Understanding 2D-BarCode Technology and Applications in M-Commerce-Design and Implementation of A 2D Barcode Processing Solution," in *Proc. of 31st Annual International Computer Software and Applications Conference*, Jul. 24-27, 2007, pp. 49-56.

[31] QR Code.com, *http://www.qrcode.com*

[32] Twit88.com, *platform.twit88.com/projects/show/mt-qrcode*

[33] L. N. Kim, S.-E. Choi, J. Kim et al., "Single exposure fabrication and manipulation of 3D hydrogel cell microcarriers" *Lab on a Chip*, vol. 11, pp. 48-51, 2011.

[34] J. W. Goodman, *Introduction to Fourier Optics 3rd edition*. ROBERTS & COMPANY, 2005.

[35] B. V. Slaugther, S. S. Khurshid, O. Z. Fisher et al., "Hydrogels in Regenerative Medicine" *Advanced Materials*, vol. 21, pp. 3307-3329, 2009.

[36] M. B. Mellott, K. Searcy, and M. V. Pishko, "Release of protein from highly cross-linked hydrogels of poly(ethylene glycol) diacrylate fabricated by UV polymerization" *Biomaterials*, vol. 22, pp. 929-941, 2001.

[37] N. A. Peppas, P. Bures, W. Leobandung et al., "Hydrogels in pharmaceutical formulations" *European Journal of Pharmaceutics and Biopharmaceutics*, vol. 50, pp. 27-46, 2000.

[38] Sigma-Aldrich Co., Material Safety Data Sheet for Rhodamine B, *http://www.sigmaaldrich.com*

국문 초록

위조제품을 이용한 범죄가 세계적으로 끊임없이 증가하고 있다. 화폐, 신분증, 약, 심지어 주류 등 여러 제품에 위조를 방지하기 위해 많은 기술들이 적용되고 있으나 위조 수법이 점점 고도화 되면서 더욱 진보된 위조방지 기술들이 요구되고 있다. 미세입자는 아주 작기 때문에 제품에 숨겨 놓았을 때 찾아내기가 어렵고 서로 다른 미세입자들을 섞어서 사용하면 더욱 위조하기가 힘들어진다. 하지만 미세입자를 이용한 위조방지 기술에 대한 연구는 많이 이루어지지 않은 상황이다. 이 학위논문에서는 코드화된 미세입자를 만들고 이를 화폐와 약의 위조방지 기술로 적용시켜보고자 한다.

화폐 위조방지에는 모양으로 코드화된 미세입자를 적용하였다. 50~500 ㎛ 크기의 폴리머 입자들을 만들었으며, 각각의 입자는 서로 다른 모양을 가지면서 내부에 특정한 문자가 새겨져 있다. 또한 서로 다른 세 가지의 형광 염료를 사용하여 모양과 함께 색으로도 정보를 제공하였다. 하지만 이렇게 제작된 폴리머 입자들은 내구성이 약하기 때문에, 제조 과정에서 오는 물리적 힘으로부터 입자들을 보호하기 위해 제작된 입자를 실리카 코팅 하였다. 두께가 15~40 ㎛ 정도 되는 실리카 코팅된 입자들은 입자의 크기에 상관 없이 종이에 잘 도입 되었다. 이처럼 종이에 도입된 미세입자는 작으면서도 모양과 형광 두

요소로 이중 코드화 되어 있기 때문에 높은 보안수준을 제공해 줄 수 있으므로 새로운 지폐 위조방지 기술로 응용 가능하다.

또한 스마트폰 어플리케이션으로 읽어낼 수 있는 큐알코드가 새겨진 미세입자를 제작하여 약의 위조방지에 적용해 보았다. 코드와 배경 색 사이에 충분한 콘트라스트를 주기 위해 형광 염료를 사용하였는데, 아크릴기가 포함된 염료를 사용하여 입자가 경화될 때 같이 경화되도록 하여 합성된 입자로부터 형광 염료가 확산되어 나오는 것을 방지하였다. 미세유체관 안에서 투사된 자외선의 전파 경로를 시뮬레이션하여, 큐알 코드화된 미세입자 생성시 코드 안쪽에 있는 고립된 구조물이 본체로부터 떨어져 나오지 않도록 코드의 모듈 크기는 40 ㎛ 이하로, 채널의 높이는 25 ㎛ 이상으로 정하였다. 제작된 큐알 코드화된 미세입자에는 버전 7 의 저장용량과 최고 수준의 오류 복원 기능을 적용했을 때 93 개의 영숫자를 기록할 수 있었는데, 이는 약의 정보를 저장하는데 충분한 용량으로 생각된다. 최고 수준의 오류 복원 기능을 적용했을 때, 입자의 데이터 저장 부분이 20%가량 손상되었을 때도 코드 해독이 가능하였다. 또한 큐알 코드에는 위치 찾기 심볼이 포함되어 있어 입자가 어떤 각도로 놓여있든 스마트폰을 돌리지 않고 해독이 가능하였다. 제작된 미세입자가 포함된 알약을 이용하여 인증 과정을 데모하였으며 세포독성 실험을 통해 미세입자가 안전함을 확인하였다. 제안된 큐알 코트화된 미세입자는 기존에 연구된 미세입자가 가질 수 없었던 고용량 코드화와 오류 복원 기능을 제공하기

때문에 약의 위조를 방지하기 위한 진보된 기술로써 유용하게 쓰일 것으로 보인다.

주요어 : 위조방지, 모양으로 코드화된 미세입자, 실리카 코팅, 큐알 코드화된 미세입자

학번 : 2011-20853